Influence of Tool Runout on Force Measurement during Internal Void Monitoring for Friction Stir Welding of 6061-T6 Aluminum

Daniel Franke¹, Michael Zinn², Shiva Rudraraju³, Frank E. Pfefferkorn^{4,*}

- 1 Department of Mechanical Engineering, University of Wisconsin-Madison, USA, email: dfranke2@wisc.edu
- 2 Department of Mechanical Engineering, University of Wisconsin-Madison, USA, email: mike.zinn@wisc.edu
- 3 Department of Mechanical Engineering, University of Wisconsin-Madison, USA, email: shiva.rudraraju@wisc.edu
- 4 Department of Mechanical Engineering, University of Wisconsin-Madison, USA, email: frank.pfefferkorn@wisc.edu

 * Corresponding author, email: frank.pfefferkorn@wisc.edu

Abstract

The goal of this research is to examine how altering the amount of friction stir tool eccentricity while controlling the amount of slant in the tool shoulder (drivers of oscillatory process forces) effects the generation of process force transients during sub-surface void interaction. The knowledge gained will help improve the accuracy of force-based void monitoring methods that have the potential to reduce the need for post-weld inspection. The eccentric motion of the tool produces oscillations in the process forces at the tool's rotational frequency, which becomes distorted when features on the probe interact with voids, generating an amplitude in the force signals at three times the tool rotational frequency (for three flat tools). A larger tool eccentricity generates a larger amplitude in the force signals at the tool's rotational frequency, which has a greater potential to create a distortion during void interaction. Once a void becomes large enough to produce amplitude at the third harmonic larger than 30% of the amplitude at the rotational frequency, the trailing edge of the tool shoulder cannot fully consolidate the void. The interaction between the eccentric probe and sub-surface void is isolated by ensuring any geometric imperfection in the shoulder (slant) is removed. The results suggest that geometric imperfections (eccentricity and slant) with respect to the tool's rotational axis must be known when developing a void monitoring method from force transients of this nature.

Keywords: friction stir welding, aluminum, internal voids, process monitoring, forces

1. Introduction

Friction stir welding (FSW) is a solid-state joining method that relies on the use of a rotating tool to plastically deform workpieces and mechanically intermix them. The deformation that occurs during the process generates thermal energy that raises the temperature of the material to 80-95% of the alloy's solidus temperature. Elevated temperatures are critical in reducing flow stress and enhancing material flow, but the fact that the material does not melt provides the process with advantages over fusion based welding of aluminum alloys. The advantages include, but are not limited to:

- Less severe heat affected zone in heat-treated aluminum alloys
- Reduction in workpiece residual stresses and distortion
- Elimination of hot cracking
- Elimination of the need for shielding gas
- Less embodied energy
- Fine equiaxed grain structure

Substantial research has shown that friction stir welding is capable of creating high-quality joints in aluminum and other lightweight alloys such as magnesium [1,2]. However, certain limitations have hindered the adoption of the friction stir welding process. Significant limitations include the need for new design of components for friction stir welding, more robust fixturing, and higher capitol costs. Additionally, the process can be limited by its tendency to form sub-surface voids as the result of a lack of material

transfer around the tool probe. The potential of sub-surface void formation is a factor in the limitation of the process in terms of travel speed, which has slowed process adoption for high volume production. When attempting to traverse through the workpiece at a high rate, it becomes harder to successfully transfer material from the leading edge of the tool probe to the trailing edge of the tool probe to be deposited in the weld. This is believed to be due to the inadequate thermomechanical state that results from trying to move a larger amount of material around the probe per revolution at the lower temperatures that are resultant of traversing faster. Inadequate material flow results in the formation of volumetric sub-surface voids in the region of the weld deformed by the probe (Figure 1). Sub-surface voids of significant size are detrimental to the strength of the joint. The potential for sub-surface void formation has also hindered the adoption of the process in high-reliability applications due to the cost of post-weld nondestructive evaluation (NDE). Developing a method of real-time internal void monitoring based on a measured process output holds the potential to increase process adoption by addressing the limitations in process speed and costly post-weld inspection.

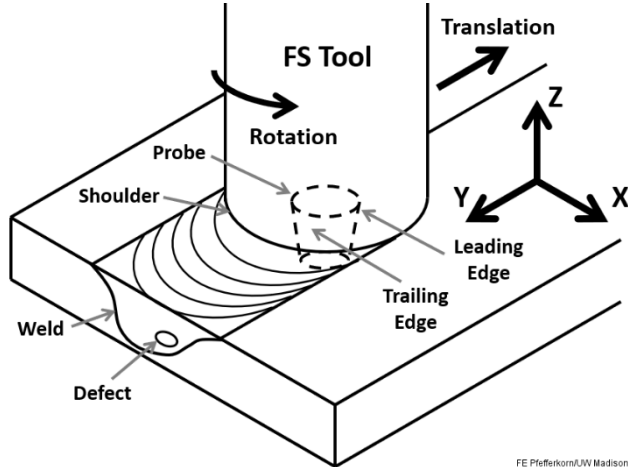


Figure 1: Depiction of the relevant aspects of the friction stir welding process. Note the 3-axis coordinate system for future reference.

Mishra et al. [3] have prepared a review paper on methods of void mitigation and control of the process for internal void avoidance. Researchers have proposed different methods of monitoring subsurface voids through the measurement of multiple different process outputs including force, torque, electrical current, temperature, vibration, and acoustic emission. A growing portion of research has focused on force and torque based measurements due to their high sensitivity to the stresses that drive the severe plastic deformation of the workpiece material. Jene et al. [4], examined the frequency content of welding forces in the plane of welding (X and Y directions) using a short time Fourier transform, and observed a distinct change in the frequency content of the force signals within voided regions of the weld. Fleming et al. [5], investigated in-process void avoidance created by workpiece gaps in robotic FSW. Through frequency analysis of the axial force signal, the authors proposed new statistical methods of interpreting axial force measurements to provide information on the condition of weld consolidation. Ramulu et al. [6], analyzed the effect of welding process parameters on the formation of sub-surface voids during FSW. A criterion was developed for predicting the onset of void formation by examining the changes in axial force and torque as a function of welding parameters. Kumar et al. [7], examined void detection of the friction stir welding process by using a discrete wavelet transform on axial force and torque signals. Their work showed that void formation produced sudden changes in the axial force signals which were best captured using the discrete wavelet transformation and a square of errors statistical tool. Kumari et al. [8], applied a continuous wavelet transformation on the measured axial force in combination with a statistical feature using the variance of scale 1 to localize voids in friction stir welds. They suggested that a continuous wavelet transform can provide better resolution than a discrete wavelet transform when it comes to void

localization. Das *et al.* [9], used wavelet analysis and the Hilbert-Huang transform to correlate measured axial loads to the formation of defects. They showed that the axial load has distinct undulations at frequencies lower than the tool rotational frequency due to a long-range breakdown in material flow. Boldsaikhan *et al.* [10], utilized a multilayer neural network and discrete Fourier transform to correlate changes in the frequency content of the process forces (X and Y directions) and the formation of continuous tunnel voids. The researchers observed amplitudes in the signals primarily at the tool rotational frequency during good welding conditions and an increase in the amplitude of frequencies both lower than and higher than the tool rotational frequency during bad welding conditions.

A common theme within the prior research on force and torque based monitoring methods involves the void formation producing changes in measured outputs at distinct frequencies. A form of frequency analysis is then used to correlate changes in forces or torques to void occurrence. However, physical descriptions as to what is occurring at the frequencies of interest when the disturbance is generated are not presented. Without the development of a physical understanding of what causes the changes in process measurements, it is hard to know when and how the method can be transferred to situations where process settings have changed. Forces and torques are highly sensitive to all aspects of the process such as the machine, workpiece geometry, workpiece alloy, tool geometry, and process parameters. When these aspects of the process change, the method of void detection has to adapt to the changes. The adaption process can be expedited if the fundamental physical mechanisms of what is causing changes in measured process outputs is understood. The goal of the current work is to further the fundamental understanding of how specific transients in measured force signals change during void interaction.

Several prior studies have shown that welding process force signals oscillate at the spindle rotational frequency when measured at a high enough sampling frequency and sensitivity [10-18]. Shrivastava et al. [18,19] showed that force signals are distorted during sub-surface void formation, which resulted in the generation of an amplitude in the measured signal at the frequency of the harmonic of the nominal spindle frequency corresponding to the number of flats on the tool probe. A correlation was developed between the amplitude of the third harmonic in the Y force signal and the corresponding volume of voids when using a three-flat tool probe, which produced a method of predicting void size from measured force transients. However, the correlation was developed for one specific tool in 6061-T6. In order to work towards extending the method to other aluminum alloys and tool geometries, a physical understanding of the source of the force oscillation at the frequency of the spindle rotation, in addition to the source of the amplitude at the third harmonic was proposed in Franke et al. [20]. An experimental apparatus was used to measure process forces within the same timing scheme as measurements of angular location of physical attributes of the tool (e.g., flats, runout, etc.). This allowed for the observation that if the tool has a substantial amount of eccentricity about its true rotational axis, the direction of the oscillatory force in the X-Y plane tends to point towards the angular position of the most eccentric part of the tool. Conversely, if the tool has a substantial amount of slant in the tool shoulder (unlevel shoulder that rotates), then the direction of the oscillatory force will lead the low point of the slanted shoulder by 90°. These two geometric imperfections appear to be the primary drivers of the oscillation in force signals during friction stir welding. When the peaks of the tool probe created by the three flats are in the same angular location as the void volume, the tool is momentarily deflected into the volume, and the oscillatory force that the runout of the tool applies to the surrounding material is momentarily reduced. This interaction (explained in detail in [20]) leads to the generation of the amplitude at the third harmonic. The current work seeks to take the foundational aspect of correlating the amplitude of the third harmonic to void size developed by Shrivastava et al. and expand upon it using the knowledge proposed by Franke et al. Specifically, the current work examines how altering the amount of tool eccentricity and controlling the amount of slant in the tool shoulder (drivers of force transients) effects the generation of the amplitude of the third harmonic during void interaction, as they are not considered in the prior work.

2. Methods

2.1. Experimental Apparatus

The apparatus utilized in the current study consisted of the same apparatus used in [20]. Friction stir bead on plate welds were produced using a 3-Axis CNC Mill (HAAS, TM-1). The transducers used to study the process include a magnetic angular encoder (HAAS, Part #: 30-30390, 1024 pulses per revolution) connected to the CNC mill spindle, and a three-axis piezoelectric force dynamometer (Kistler, model 9265) on top of which workpieces were mounted. Force dynamometer change signals were fed to charge amplifiers, which in turn sent the amplified force signals to the data acquisition system (National Instruments, BNC-2090A, PCI-6014, PCIe-6320) along with the encoder output from the optical isolator (AutomationDirect, FC-ISO-C) downstream from the encoder. The dynamometer captured three force signals in the three directions labeled in Figure 1. The workpiece fixture on top of the dynamometer is designed to hold the workpieces at a three-degree travel angle with respect to the tool since the spindle is oriented with the Z direction and fixed. This means the workpiece is rotated three degrees and the tool is programmed to move along the three-degree angled path of the workpiece surface in order to achieve this travel angle during the welding process.

2.2. Friction Stir Tools

The same friction stir tools examined in [20] were examined in the current work. The three tools examined were nominally the same (Figure 2), consisting of a concave shoulder (15 mm diameter) and a 5.1 mm long probe (7 mm in diameter at shoulder tapered to 5 mm in diameter). Each probe had three flats machined into the surface spaced at 120° apart with a constant depth of 0.625 mm. The probe was threaded with a constant thread depth of 0.625 mm at a 1 mm pitch. Each tool varied in terms of its natural runout when mounted in the machine spindle. The runout of each specific tool is resultant of how the tool is machined and how it is held in the tool holder as described in detail in [20]. The kinematic runout of each tool while rotating within the machine spindle was measured with a dial indicator with a resolution of 2.5 µm. The runout measurement encompasses circularity and eccentricity, but since the tools are turned on a lathe, the circularity of the tool's surface was assumed to be insignificant compared to eccentricity. The shoulder surface (that contacts the workpiece) of each tool was machined perpendicular to the rotational axis of the milling machine by turning the surface using the mill spindle as described in [20]. This leaves only the eccentricity as a major geometric imperfection (Table 1) that rotates with the tool and generates force oscillations [20].

Table 1: The measured kinematic true runout of each tool

	Tool 1	Tool 2	Tool 3
Runout	46 μm	74 μm	183 μm
	(0.0018 in)	(0.0029 in)	(0.0072 in)

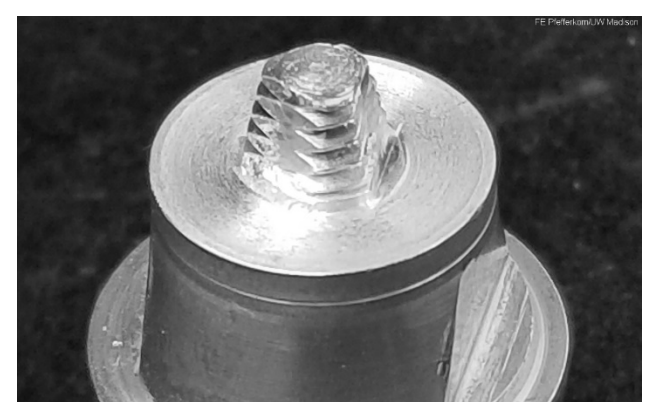


Figure 2: Image of the features (flats and threads) on the probe of one of the friction stir tools used in the study.

2.3. Experimental Procedure

The workpieces utilized for all welds consisted of aluminum 6061-T6 plates that measured 203 mm (8 inches) in length (Y), 102 mm (4 inches) in width (X), and 6.35 mm (0.25 inches) in thickness (Z). The welds were produced with a 3-degree travel angle of the tool, and to a total weld length of 150 mm. The backing material consisted of a 6.35 mm thick plate of mild steel. The welds were programmed with a shoulder plunge depth of 0.2 mm (position control) at the center of the tool shoulder (in the travel angle direction). However, the compliance of the system resulted in the tool shoulder center located near the surface of the workpiece during the steady-state portion of the welding process. The welding parameters were altered to produce welds that ranged from fully consolidated conditions to void producing conditions. This was achieved by incrementally increasing the advance per revolution (APR) of the weld by increasing the travel speed at the set rotational speeds of 800, 1000, and 1200 rpm. The full set of welding parameters that were performed with each of the three tools is listed in Table 2. The largest three APR conditions were not performed for Tool 3 since that specific tool started to form substantially large voids at a lower advance per revolution conditions than Tools 1 and 2. This resulted in 54 total bead on plate welds being generated with all three tools.

Table 2: Spindle speeds and feed-rates (i.e., advances per revolution) used to create voided and fully consolidated welds for all three tools.

		Spindle Speed		
		800 rpm	1,000 rpm	1,200 rpm
	0.3 mm	240 mm/min	300 mm/min	360 mm/min
er n	0.4 mm	320 mm/min	400 mm/min	480 mm/min
e P Itio	0.5 mm	400 mm/min	500 mm/min	600 mm/min
olu	0.6 mm	480 mm/min	600 mm/min	720 mm/min
Advance Per Revolution	0.7 mm	560 mm/min	700 mm/min	840 mm/min
A B	0.75 mm	600 mm/min	750 mm/min	900 mm/min
	0.8 mm	640 mm/min	800 mm/min	960 mm/min

Three cross-sections (in the X-Z plane) were cut from each weld. The cross-sections were cut near the center of the weld with 15 mm between each cross-section. The collected force data confirmed that the friction stir welding process was at a steady state (with regard to the average process forces) at the center position of the weld where the sections were cut. The distances of the cross-section locations from the start and end of the weld (in terms of where the trailing edge of the tool probe resides at each position) were measured with an estimated uncertainty of ± 1 mm. These distances were then used to locate approximate points in time within the force data by examining where the force in the travel direction (Y direction) spiked at the start of the weld (designates start time corresponding to the zero position) and dropped rapidly at the end of the weld (designates end time corresponding to 150 mm position). A linear relationship between position and time was used to calculate the time within the force data that the trailing edge of the tool probe would reside at the position of the cross-section. At each of the three corresponding approximate points in time, a discrete Fourier transform was applied over three tool rotations (three cycles per cross section) in order to extract the frequency content of the X and Y direction force signals with respect to the tool rotational frequency. This method relied on the assumption that the void size and force transients are relatively consistent over several adjacent advances per revolution of the tool. This would allow the three force cycles that span the region of weld from which the cross sections were cut to represent the void size observed. The average force value that the FS tool applies to the surrounding material (about which the signals oscillate) was also calculated from the same force data over which the frequency content was extracted.

2.3.1. Measuring Internal Void Size

The cross-sections from all welds were ground and polished to reveal the two-dimensional nature of the voids within each cross-section. White light optical microscopy (Alicona InfiniteFocus G4, Graz, Austria) was used to produce an image of all voids from which an area value was extracted by means of a custom image analysis program written in Mathworks MATLAB. Black and white version of the void

images were segmented using a threshold pixel value of 200. Subsequently, image cleaning was applied in order to convert any artifacts that can fit inside a 5-pixel diameter circle to the surrounding medium. A direct relationship between the number of pixels in the scale bar and the number of pixels within the void region was used to calculate the area of the void region.

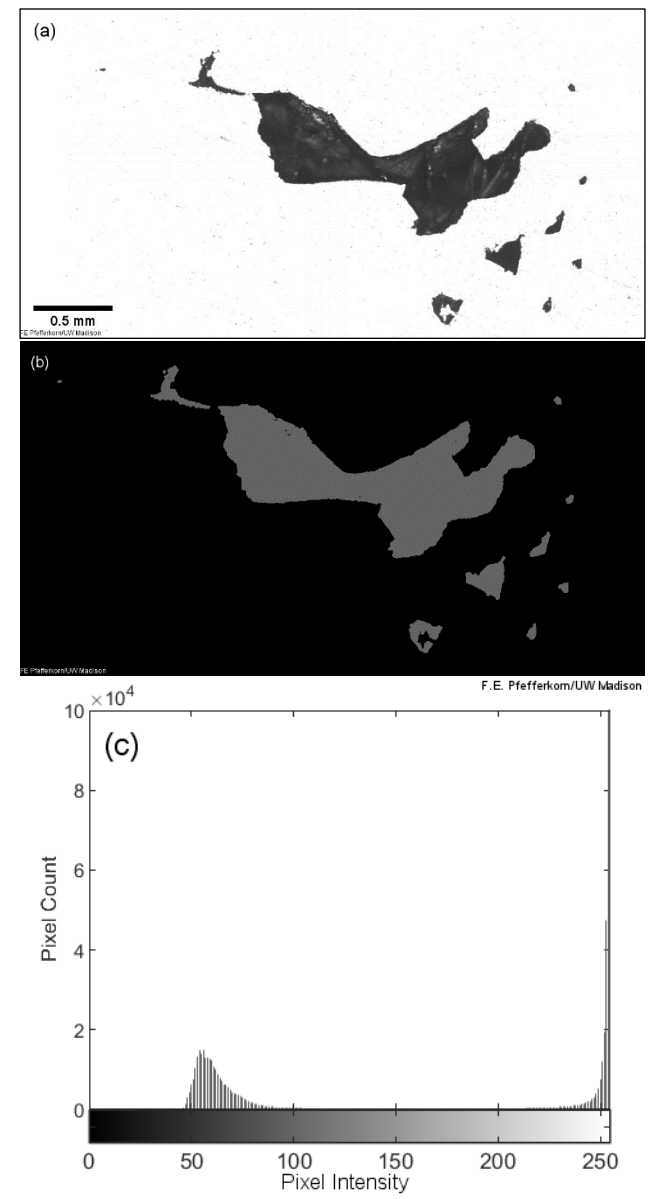


Figure 3: Depiction of Image analysis method: (a) white light image of void, (b) segmented image used for area measurement, and (c) histogram of image.

2.3.2. Computed Tomography Imaging of Representative Internal Voids

Four welds that contained voids and one fully consolidated weld (as determined by the cross sections) were selected for further three-dimensional computed tomography (CT) imaging to reveal the three-dimensional nature of the voids created in this study. The welds were selected based on the void cross-sectional area and the tool used. Two of the welds with voids were created by Tool 1, one with void areas at the large end of all of the welds created by Tool 1, and one with void areas towards the small end of the range of areas. Similar welds on the large and small end of void sizes were chosen for Tool 2. The samples

consisted of 15 mm sections of weld that were cut from 100-115 mm along the total weld length. All samples were scanned on a Siemens Inveon microCT (Siemens Medical Solutions USA, Inc., Knoxville, TN) utilizing the following parameters: 80kVp, 1,000 µA current, low magnification, bin factor 2, 1.5mm aluminum filtration, 1050ms exposure time, and 600 projections over 220 degrees. Raw data was reconstructed with filtered back-projection by applying the Shepp-Logan filter using the high-speed COBRA reconstruction software (Exxim Computing Corporation, Pleasanton, CA) yielding isotropic voxels of approximately 31.52 microns. The scans were analyzed in the Inveon Research Workplace software. All CT scan datasets were evaluated using threshold values ranging from -700 to 1,000 Hounsfield units.

2.3.3. Measuring Resultant Tool Plunge Depth

An optical profilometer (Alicona InfiniteFocus G4, Graz, Austria) was used to scan the surface of all welds to measure the position of the surface of the weld relative to the initial workpiece surface. All scans were taken with a 5X magnification lens and a vertical scan resolution of 1 μ m. All scans were taken across the weld at the position adjacent to the last cross section cut from the weld (15 mm along the weld length after last cross section). A profile (Figure 4) was extracted from each scan by averaging the height data within a 1 mm band across the weld in the Profile-Form Measurement module within the Alicona IF Measure Suite software. The step height from the top surface of the workpiece to the bottommost point of the weld surface was measured. This measurement gives an approximate vertical location of the trailing edge of the tool shoulder during welding.

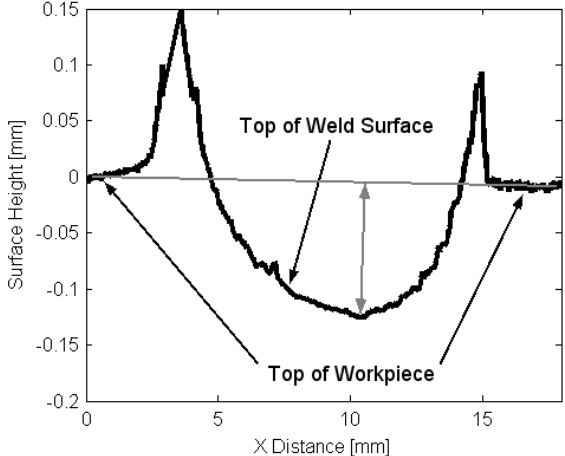


Figure 4: Example surface profile taken from the profilometer scan of a weld surface.

3. Results and Discussion

The objective of any force-based monitoring method is to correlate a change in measured forces with the occurrence and size of voids. The most distinct change observed in the process forces (when using a three-flat tool) is the generation of an amplitude at the third harmonic of the tool rotational frequency due to the distortion in the oscillating force signals described in [20]. It has been proposed that tool runout applies a dynamic force to the workpiece each revolution, which generates the oscillations in the measured forces with a frequency corresponding to the nominal tool rotation rate. When two of the peaks of the tool probe (created by the three flats) each separately interact with a void volume, the interaction produces a momentary reduction in the amplitude at the tool rotational frequency due to the lack of contact. The distortions in the amplitude at the tool rotational frequency can be extracted as an amplitude at the third harmonic when looking at the frequency content of the signal.

3.1. Force Transients Measured Perpendicular to Welding (X-direction)

The primary objective of the current research is understanding how altering the runout of the tool alters the relationship between the amplitude of the third harmonic and void size. Each cross-sectional void area is plotted against its corresponding amplitude at the third harmonic in the X-direction force signal for all three tools in Figure 5. The relationships for Tools 1 and 2 (Figure 5 (a) and (b)) show similar trends. First, there is a distinct cutoff value between the fully consolidated welds and welds containing internal voids in terms of the amplitude of the third harmonic. Secondly, the void areas appear to grow exponentially with an increase in the amplitude of the third harmonic. This suggests that after a certain void size is reached, the amplitude of the third harmonic reaches a pseudo saturation limit. The cutoff values between full consolidation and void presence and the saturation limit are both larger for Tool 2, which had a larger kinematic runout. The larger runout also generated larger force amplitudes at the nominal rotational frequency of the tool during a welding condition with full contact between the probe features and the workpiece, i.e., no void interaction. During a weld with no void interactions (1,000 rpm and 200 mm/min), when the force oscillations were purely at the tool rotational frequency (no substantial amplitudes at higher harmonics), Tool 1 generated an amplitude at the tool rotational frequency of 140 N in the X direction, whereas Tool 2 generated an amplitude of 180 N [20]. These two values have been plotted as vertical lines at the far-right end of each respective plot. The cutoff value for the amplitude of the third harmonic that differentiates fully consolidated welds from welds with voids in the cross-sections is approximately 30% of the respective amplitude at the fundamental frequency in a full-contact welding condition for both Tool 1 and Tool 2. Additionally, the saturation limit value is approximately 70% of the amplitude at the tool rotational frequency for a full-contact weld. It makes physical sense that the amplitude of the third harmonic saturates at a value less than that of the amplitude at the tool rotational frequency because it appears that the amplitude at the third harmonic is manifested through a reduction in the amplitude at the tool rotational frequency due to a reduction in contact between the probe features and workpiece material. Maximum contact between the probe and surrounding material leads to the maximum force amplitude at the tool rotational frequency in a full-contact welding condition, of which the amplitude of the third harmonic should not be larger than due to less contact. A depiction of how the amplitude at the tool rotational frequency devolves into a saturated amplitude at the third harmonic is illustrated in Figure 6.

The trends observed for Tools 1 and 2 do not extend to Tool 3 (largest kinematic runout), which can be observed in Figure 5 (c). This is due to the different flow mechanisms produced by Tool 3 as described in [20]. The larger runout of Tool 3 resulted in void formation at lower advance per revolution conditions than with Tools 1 and 2. Additionally, the voids generated by Tool 3 were larger across the comparative parameter space studied. It has been proposed that the excessively large runout of Tool 3 displaces material from the weld zone as opposed to shearing is around the probe to be deposited in the weld. This displacement mechanism appears to mask the reduction in force when a peak on the tool probe interacts with a voided volume. This results in relatively small third harmonic amplitudes at relatively large void sizes when compared to the relationships observed for Tools 1 and 2. The flow condition produced by excessive eccentricity should be avoided in a production setting. It would be harder to develop a force transient based monitoring method, and such tool conditions would tend to cause voids at less aggressive process parameters. This suggests the magnitude of the friction stir tool's runout relative to the tool's total size needs to be considered to avoid this type of material transfer.

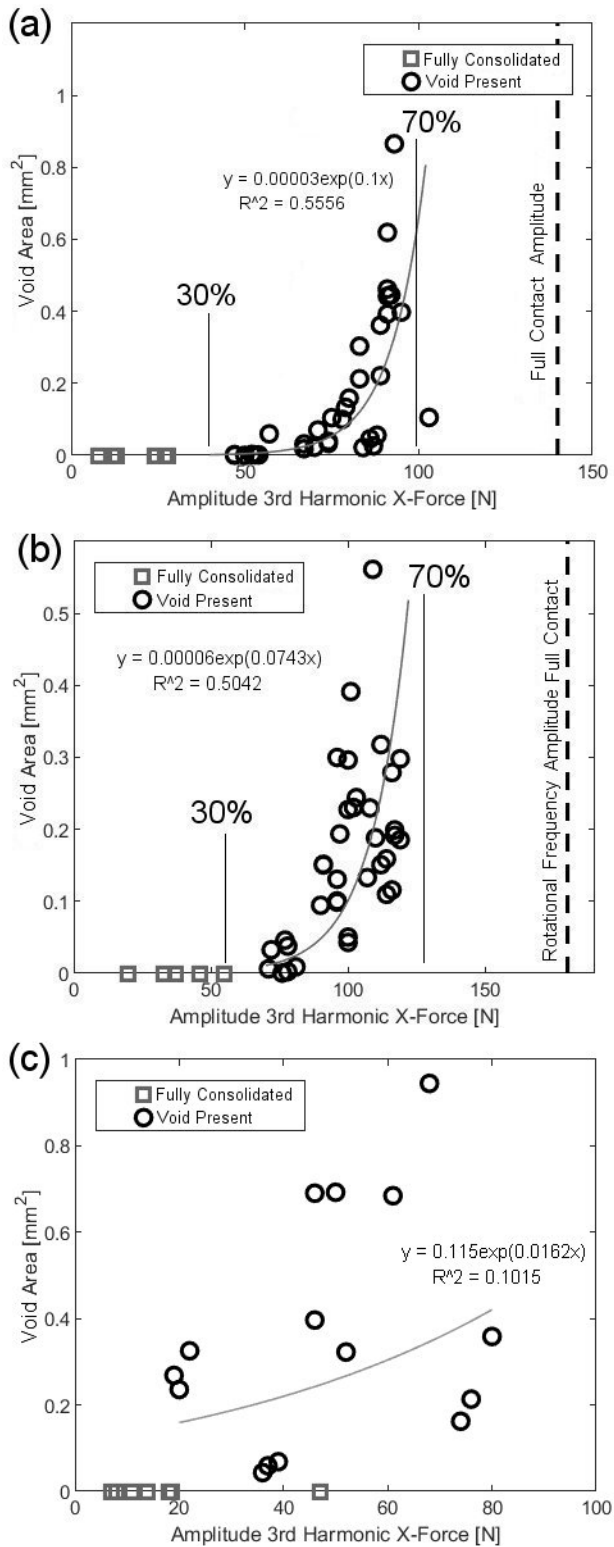


Figure 5: The relationships between measured third harmonic X-direction force amplitudes and void areas: (a) Tool 1, (b) Tool 2, and (c) Tool 3.

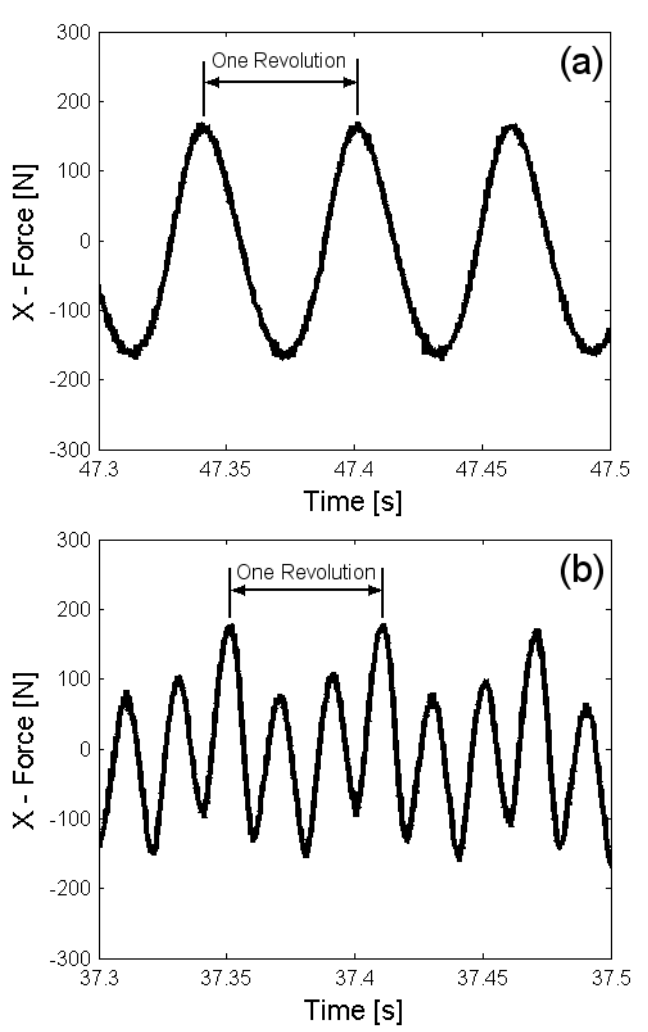


Figure 6: Force signals in X direction during welds performed with Tool 2: (a) welding condition with full probe/material contact within each revolution, (b) distorted signal due to a reduction in material contact leading to an amplitude at the third harmonic that has saturated at 70% the amplitude in the full contact condition. Note: the average force in this X direction has been removed from the signal, *i.e.*, it is normalized around zero.

3.2. Force Transients in the Direction of Welding (Y-direction)

Similar trends to X-direction forces can be observed in the relationships between the amplitude of the third harmonic in the Y-direction and void size (Figure 7). The amplitudes at the tool rotational frequency in the Y-direction tend to be larger than the amplitudes in the X-direction for a given weld. This is due to the eccentric motion adding to the bulk travel motion of the tool. The larger amplitudes in the Y direction during a fully consolidated weld are plotted as vertical lines at the right end of the plots for Tools 1 and 2 in Figure 7 (a) and (b). The amplitudes of the third harmonic for welds with voids fall within a similar 30-70% range that was previously observed in the X-direction trends. However, there appears to be a larger spread of the data points about the exponential fit as described by the smaller R-squared values. It is hypothesized that the trends are affected by larger variations in the average force values in the Y direction.

Within the steady state portion of all welds, the tool applied an average force to the workpiece in the negative Y-direction in Figure 1(travel direction), and an average force in the negative X-direction in Figure 1(due to the shearing that occurs in front of the tool). The force transients in the X and Y directions oscillate around the aforementioned average force values. It has been hypothesized that the magnitude of the average force impacts the magnitude of momentary deflection of the tool into voided volumes during interaction [20]. A larger average process force will drive the tool to deflect more when an imbalance in the pressure field around the probe is created by the presence of a voided volume. The larger deflection and/or pressure file generates a larger distortion in the force signal. Across the welding conditions studied, the average forces in the X-direction ranged between 577 and 1471 N with a standard deviation of 276 N for Tool 1 and ranged between 1103 to 1951 N with a standard deviation of 262 N for Tool 2. In the Y-direction signals, the average forces ranged between 1798 and 3857 N with a standard deviation of 582 N for Tool 1 and ranged between 1717 and 3561 N with a standard deviation of 474 N for Tool 2. There is an approximate doubling in the range and standard deviation when comparing the X-direction average forces to the Ydirection average forces. This coincides with a reduction in the R-squared values of the exponential trends by an approximate factor of two when comparing the Y-direction trends to the X-direction trends. This suggests that since the driving force for momentary tool deflection into voids is more consistent in the Xdirection, it becomes the ideal direction for measuring a force signal that can be used for predicting void size from changes in force transients. However, utilizing both signals does provide more information, and the implementation of a force measurement system from the tool side of the process may consist of a rotating coordinate system in the X-Y plane.

3.3. Force Transients in the Axial (Z) Direction

The axial (Z-direction) force is typically the largest force during friction stir welding, and therefore is often the force measurement of interest. However, it has been hypothesized that the most substantial force distortions occur in the X and Y-directions because the eccentric motion of the probe, and thus the interaction of probe features with voids, occurs in said plane. Since all welds in the current study were performed at a three-degree travel angle, there is an oscillation generated in the Z-direction force signal generated by the runout of the tool. The three-axis coordinate system is defined by the dynamometer, which is aligned with the Z-axis of the tool/spindle. The workpiece itself is tilted at three degrees from the tool and dynamometer. The oscillation in the Z-direction formed because more pressure under the tool shoulder is generated when the most eccentric point of the probe was in the trailing direction of the process (resided deeper in the workpiece). There appears to be a momentary reduction in this pressure when a peak of the tool probe interacts with a void under the trailing surface of the tool shoulder. This also generates an amplitude at the third harmonic in the Z-force signal. However, for welds where the most severe void interactions were observed (when X and Y amplitudes of the third harmonic are on the order of 100 to 150 N) the amplitude of the third harmonic in the Z-force only reached maximum values on the order of 50 N. The magnitude of the average force measurements in the Z-direction (for the parameters studied) was on the order of 10,000 N. In the plane of welding (X and Y), the magnitudes of the average force measurements were on the order of 1,000 to 3,000 N. This means that the signal to total measurement ratio is reduced by approximately a factor of 10 in the Z-direction as compared to X or Y-directions. The results suggest that it may be possible to develop a force transient void monitoring method using Z-direction force signals, e.g., if it is the only force measurement available. However, it appears that a Z-direction method would result in a reduction in sensitivity when compared to a method based on force measurements in the X-Y plane.

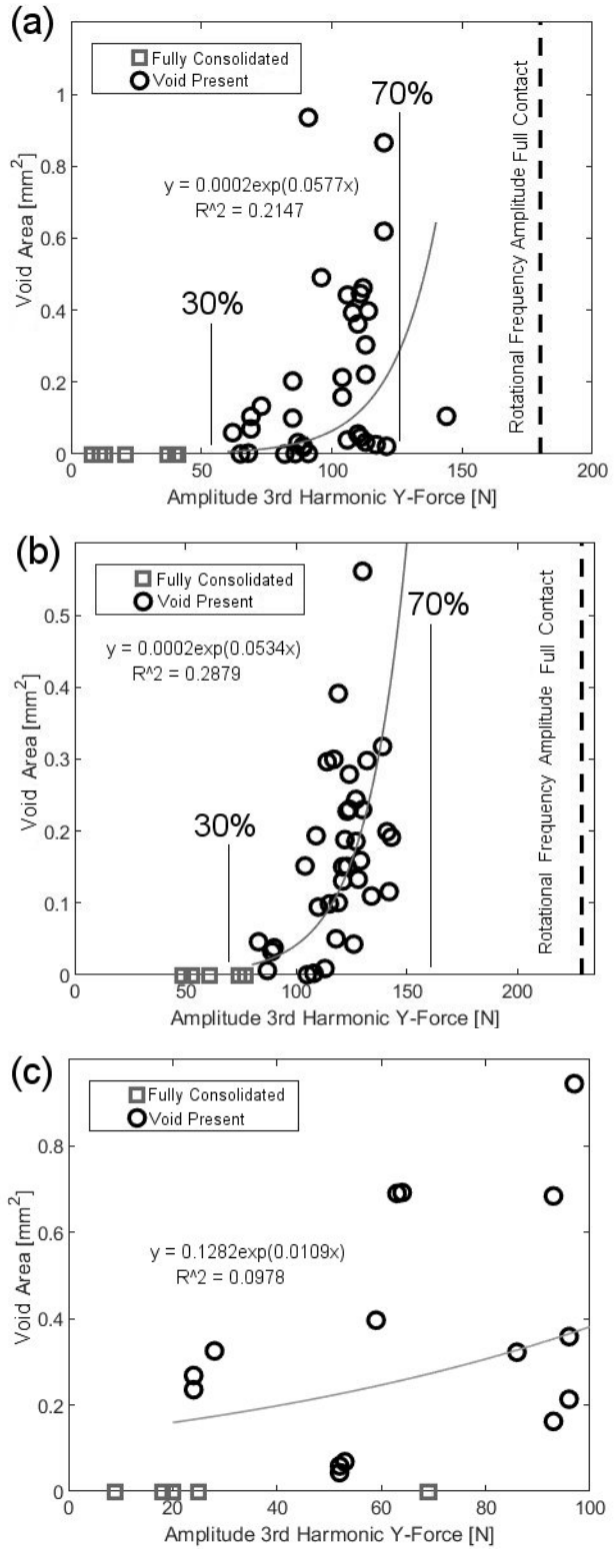


Figure 7: The relationships between measured third harmonic Y-direction force amplitudes and void areas: (a) Tool 1, (b) Tool 2, and (c) Tool 3.

3.4. Forging of Voided Volumes by the Trailing Tool Shoulder

One benefit of using a travel angle during friction stir welding is that it allows the trailing edge of the shoulder to provide additional forging and consolidation of the material in the wake of the probe. There are two main consolidation processes during friction stir welding (Figure 8), forging of material around the probe in a rotational manner, and the subsequent forging of the material downward by the trailing shoulder. This concept is relevant to the current work because the distortion in the process forces describes an interaction between the probe and workpiece material, i.e., it only describes a breakdown in the probe forging process (Process 1 in Figure 8). One limitation of the method is that it does not capture how the forging action of the trailing shoulder (Process 2 in Figure 8) affects the size of voids that may have formed during Process 1. This explains why there can be significant amplitudes of the third harmonic (breakdown in probe driven flow causing void interactions) for welds that end up becoming fully consolidated in their final state when sectioned. For example, there are amplitudes of the third harmonic of up to 60 N and 77 N (X and Y directions, respectively) for fully consolidated welds performed by Tool 2 (refer to Figures 5 (b) and 7 (b)). A void was not observed in the final weld because the forging action of the trailing shoulder compensated for the lack of material flow around the probe that resulted in the distortion of the force signals. The trailing shoulder was not able to fully consolidate the void once the void became large enough to create an interaction with the tool that generated an amplitude at the third harmonic greater than the 30% cutoff value observed.

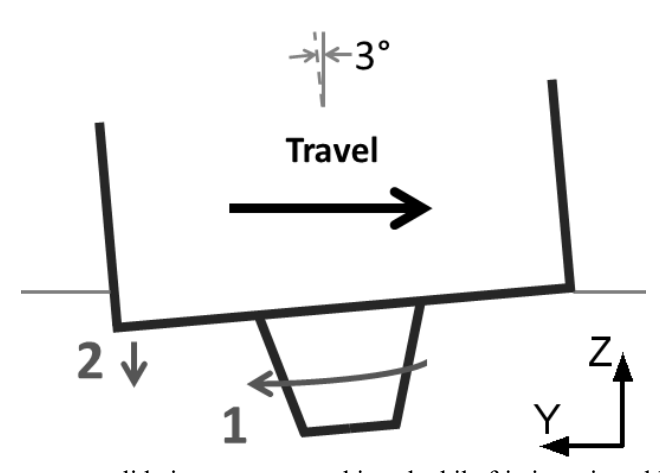


Figure 8: Depiction of the two consolidation processes achieved while friction stir welding with a 3° travel angle.

Considering the forging action of the trailing shoulder, the shoulder must have a consistent plunge depth for the relationship between the force amplitudes of the third harmonic and void sizes to be consistent. This was exemplified by one specific weld in the study in which the weld surface profile measurement revealed that the tool shoulder did not achieve a plunge depth into the workpiece surface. When examining the surface profile measurements of all of the welds performed with Tool 1, the bottommost point of surface of the weld (corresponding to the vertical position of the trailing edge of the tool shoulder), ranged between 22 and 78 µm (37 µm average with a standard deviation of 22 µm) below the top surface of the workpiece (refer to Figure 4). However, due to experimental error, in one particular weld performed with Tool 1, the trailing edge of the tool shoulder resided at a position above the top surface of the workpiece producing a surface profile measurement in which the top of the weld surface was 20 µm above the surface of the workpiece. The void area measurements from this specific weld are circled in Figure 9. Uncharacteristically large void areas are present in the final weld cross-sections due to a lack of forging by the trailing edge of the shoulder. This suggests that adding a method of controlling plunge depth (e.g., force control) has the potential to produce more consistent results in terms of predicting void size from force transients. The variance observed in the measured resultant plunge depths is a potential contributor to the spread of the data points about the exponential fits (Figures 5 and 7). Additionally, if a deeper tool plunge depth can be

achieved (*e.g.*, by using a stiffer machine) the relationships observed for the current welding parameters may have to be adapted. A larger plunge depth will change the material flow process as a whole, but it will also provide a greater ability to consolidate voids after they have formed behind the tool probe, which may cause the 30% cutoff value to shift upwards.

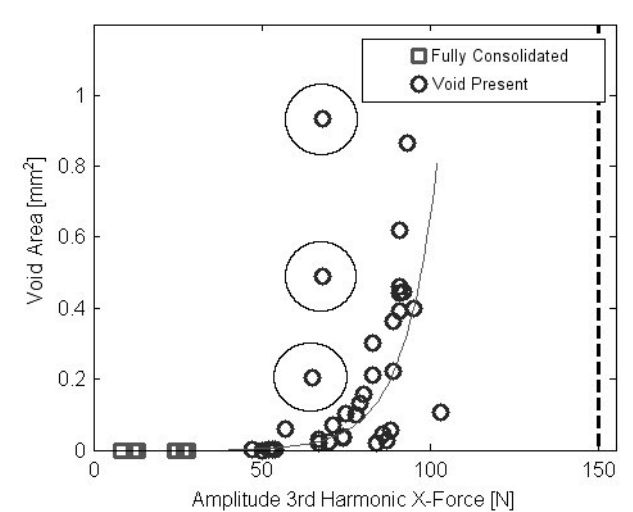


Figure 9: Abnormally large void areas (circled) due to insufficient plunge of the trailing shoulder during a specific weld performed with Tool 1.

3.5. Application of the Detection Method

Application of the method would involve extracting the amplitude of the third harmonic from the X and Y force signals, comparing them to the 30% cutoff value for the particular tool to determine whether the weld is fully consolidated or not, then using the exponential relationships to estimate the size of the void. A prediction of void size is important because small voids can be considered acceptable if they do not affect function. Within the current state of understanding, the exact trends can be assumed to be valid only for the current welding setup, i.e., using the same machine and tool geometry while welding in aluminum 6061-T6. The geometrical properties of the tool probe will also influence the force transients generated during void interaction. Deeper flats (which create sharper peaks) may possess a greater potential to react with smaller void volumes. The depth of threads on the tool probe will also affect how the features interact with a void. Geometric effects on force transient generation will need to be addressed in future research in order to fully understand the process. Additionally, the effect of different workpiece alloys on the force transient generation process needs further study. Different material properties of different alloys produce different resultant process forces under the same commanded process parameters. Preliminary work by Franke et al. [22] has proposed that aluminum alloys with higher hot strength produce larger average process forces during welding. The larger average process forces correspond to a higher pressure in the material around the tool probe. Within the higher pressure field, the effect of the disturbance created by the presence of a void will be amplified. The momentary deflection and force generation will also be dependent on the stiffness and dynamics of the machine that is used. Further details on the stiffness of the system examined in the current work can be found in [20].

The current study is a continuation in the understanding of the method proposed in Shrivastava *et al.* [18]. The prior work utilized the normalization of the amplitude of the third harmonic by the amplitude at the tool rotational frequency of the given force signal to produce a value that could be used to differentiate between voided and fully consolidated welds. It was determined that a weld contained a void when the normalized value became larger than 0.2. This normalization was utilized because examination of the amplitude of the third harmonic alone did not provide a strong differentiation. Additionally, the void size prediction model involved a relationship between the amplitude of the third harmonic normalized by the average Y-force and the size of the void normalized by a pseudo volume of sheared material based on the

advance per revolution. The major difference between the current and prior work is that the geometric imperfections of the tool (runout and shoulder slant) were not considered previously. It is hypothesized that the tool used by Shrivastava et al. had a slanted shoulder surface that rotated with the tool. The shoulder is the primary driver of the force oscillation when a significant slant in the shoulder surface is present [20]. In the current work, the shoulder slant was removed by turning the shoulder while the tool was rotating in the spindle of the machine on which friction stir welding was performed. In the prior work, the amplitude of the third harmonic was never larger than 55% of the amplitude at the tool rotational frequency for a given force signal during void interaction, i.e., the primary component of the signal remains at the tool rotational frequency. It appears that the larger amplitude of the signal at the nominal rotational frequency of the tool is driven by an unbalanced shoulder surface. The more significant reaction at the tool shoulder surface masks the interactions with the voids that form at the probe level. In the current work, the amplitude of the third harmonic became the primary component of the force signal, i.e., much larger than the amplitude at the tool rotational frequency within the signal. This can be observed in the signal shown in Figure 6 (b), where the primary amplitude of the signal is at the third harmonic with an amplitude of 80 N, while the component of the signal at the tool rotational frequency is only 20 N. The elimination of the shoulder slant in the current work appeared to isolate the probe/void interaction by isolating the effect of the probe's eccentric motion on the oscillatory forces at the tool rotational frequency. This isolation appears to provide a more direct relationship between the amplitude of the third harmonic and the void size.

3.6. Discussion of Experimental Method Assumptions

Cross-sectional area measurements of void areas are the most accessible way of quantifying void size. However, using an area measurement to describe a volumetric entity will introduce experimental uncertainty. In this analysis, it was assumed that voids were generated each revolution and that once the weld has reached a steady state, the void formation process remained relatively consistent over several advances per revolution. It is not readily achievable to match a singular void volume within the resultant weld to a singular oscillation in the force data. Therefore, several force cycles were used to calculate the frequency content, and a cross-sectional area was extracted from the length of the weld corresponding to those force cycles. The volumetric nature of the voids was examined using X-ray computed tomography (CT) datasets of selected welds in order to determine the consistency of the void size over several revolutions (Figure 10). The observed features at the distance of the advance per revolution confirm that the voids are formed on a per revolution basis. However, even at the smaller end of the void size range for both tools (Figure 10 (a) and (b)), the voids stack together to create a semi-continuous trench in the welding direction. This suggests that when sectioning the welds perpendicular to the travel direction a representative volume will be exposed regardless of the exact position along the weld length. The representative area will vary depending on the exact position of the section plane within each advance per revolution. The variation within these sections is illustrated in Figure 11. It can be observed that different sections from a singular weld expose void areas on similar orders of magnitude to each other and distinguishable from welds at different process parameters. The variation introduced by the sectioning method is a contributor to the large spread in the data shown in Figures 5 and 7. This effect appears to be most significant in the larger voids created with Tool 1, as the voids appear more discontinuous (Figure 10 (c)). It appears that the largest voids created by Tool 2 (Figure 10 (d)) tend to be more continuous than the largest voids created by Tool 1 when comparing the morphology of each. The effect of the larger eccentricity of Tool 2 on material flow appears to affect the morphology of the voids by causing them to become more tunnel-like, i.e., it created a more consistent material flow pattern per revolution.

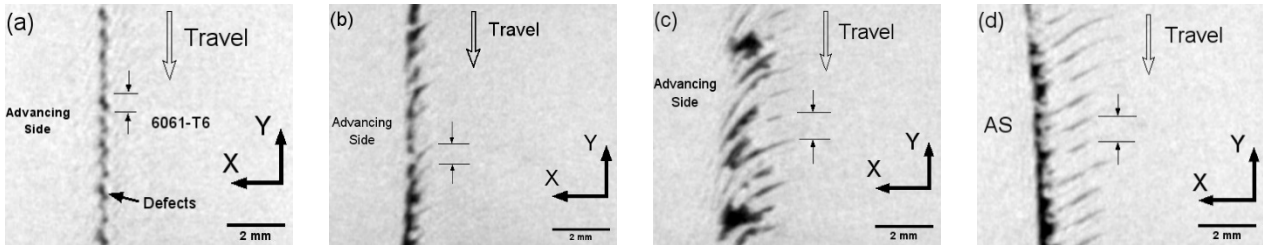


Figure 10: Images in the plane of welding extracted from CT datasets at the vertical positions (2-2.5 mm below top surface of welds) corresponding to the major volume of the voids within each weld: (a) small voids created with Tool 1, (b) small voids created with Tool 2, (c) large void created with Tool 1, (d) large voids created with Tool 2. Note that the advance per revolution of each weld is distinguished by the horizontal lines and arrows.

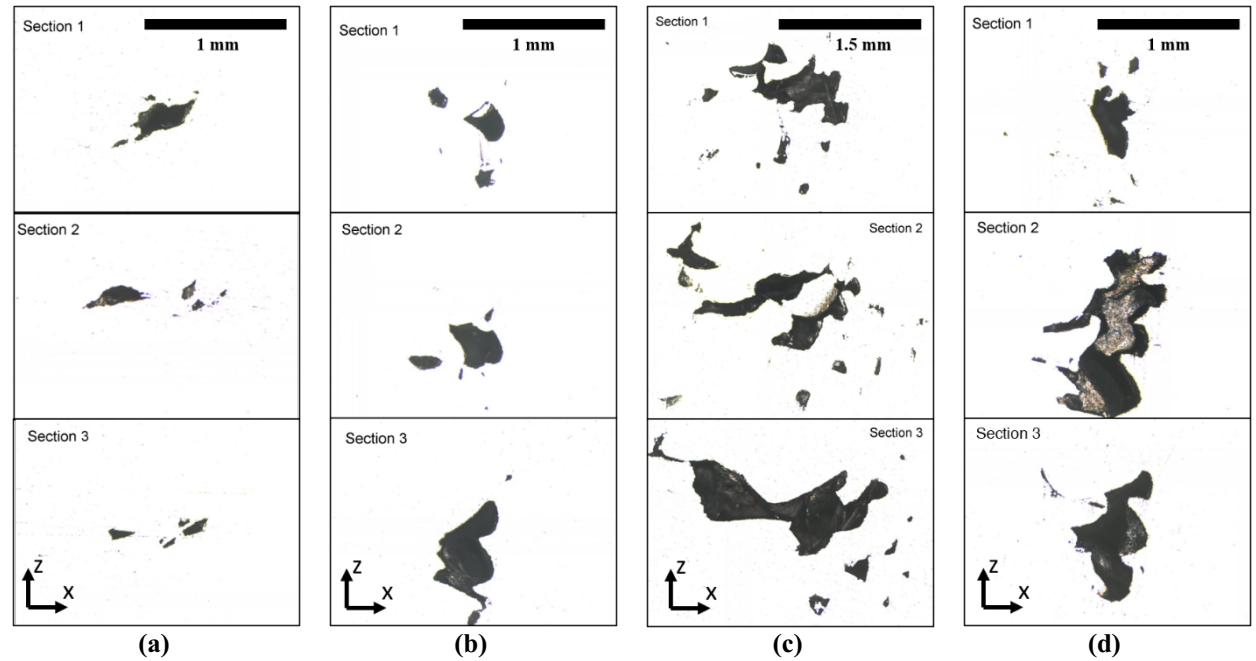


Figure 11: Three cross sections from within a singular weld at varying weld length positions: (a) small voids created with Tool 1, (b) small voids created with Tool 2, (c) large void created with Tool 1, (d) large voids created with Tool 2.

The focus of this research is the correlation of void size to changes in process force amplitudes. Prior work using the current force data acquisition system utilized a root sum square method to estimate an uncertainty of ± 8.4 N and ± 9.4 N in the measurement of the forces in the X and Y direction, respectively [18]. All force signals in the current work contained a background noise at a primary frequency of 1,000 Hz. The source of this noise is unknown. However, the amplitude of the noise never exceeded 5 N in the force signals used in the current analysis. This noise level is an order of magnitude smaller than the amplitudes that are generated at the third harmonic during welds with voids. Additionally, the frequency is on the order of magnitude larger than the highest frequency of interest in this work which is the 60 Hz corresponding to the third harmonic of the 1,200 rpm cases.

4. Conclusions

Variations in tool runout (on the order of 10's of μm) have a measurable effect on the force transient/void size relationship. This suggests that tool runout must be known and accounted for when implementing a monitoring method derived from the oscillatory force transients described. Additionally, it appears that removing the slant in an unlevel tool shoulder serves to isolate the interaction between the probe applied force and sub-surface voids. Therefore, any uneven nature of the tool's shoulder surface must be known and addressed as well. The detailed conclusions from the research are summarized as follows:

- The force amplitudes corresponding to the third harmonic of the tool rotational frequency grew in the measured X, Y, and Z directions with a positive correlation to the growth in sub-surface void size. However, the growth is more significant in the X-Y plane because the eccentric motion of the tool per revolution occurs in said plane.
- For the range of tool shoulder plunge depths studied, a void remains in the final weld once the amplitudes of the third harmonic in the X and Y directions exceed approximately 30% of the amplitude at the tool rotational frequency from a full tool/workpiece contact welding condition with no interaction.
- Once the voided volume becomes large enough (relative to the process), the amplitudes of the third harmonics saturate around 70% of the amplitude in the force signals at the tool rotational frequency during a full contact welding condition with no void/tool interaction.
- The correlation between the third harmonic and void size is strongest in the X-direction measurement because the average process force around which the transients oscillate is more consistent than in the travel direction.
- Excessive tool probe eccentricity masks the generation of the amplitudes at the third harmonic. The tool motion appears to displace material from the weld nugget as opposed to shearing it around the tool. Practitioners of friction stir welding should consider the magnitude of tool runout relative to tool size. Based on the current results as well as results from Yuquing *et al.* [23], the runout becomes excessive when its magnitude is larger than 1% of the tool shoulder's diameter when the shoulder diameter is approximately twice the probe diameter.
- Forging of the voided volume by the trailing shoulder of the tool must be controlled or monitored as the force interaction only describes the condition of the void as it interacts with the probe. Additionally, achieving a substantial plunge depth of the trailing shoulder of the tool into the workpiece can help reduce the size of subsurface voids, *i.e.*, the forging action (Process 2) shown in Figure 8 must be considered by practitioners.

Future studies on the advancement of the method will examine the effect of tool geometry (depth of flats and threads), the effect of different alloys, the effect of different machine dynamics (*e.g.*, stiffness), and the potential use of different frequency analysis methods (*e.g.*, wavelet analysis for time localization of void position along the length of the weld).

5. Acknowledgments

The authors acknowledge financial support for this research by the National Science Foundation grant CMMI-1826104. Additionally, the authors acknowledge the University of Wisconsin Carbone Cancer Center Small Animal Imaging and Radiotherapy Facility (SAIRF) [Support Grant P30 CA014520]. The authors would also like to acknowledge Friction Stir Link Inc., the Department of Mechanical Engineering at the University of Wisconsin Madison, and the Machine Tool Technology Research Foundation.

References:

- [1] Mishra RS, Ma ZY. Friction Stir Welding and Processing. Mater. Sci. Eng:R:Reports 2005:50:1-78. https://doi.org/10.1016/j.mser.2005.07.001
- [2] Threadgill PL, Leonard AJ, Shercliff HR, Withers PJ. Friction Stir Welding of Aluminium Alloys. Int. Mat. Rev. 2009:54:49-93. https://doi.org/10.1179/174328009X411136
- [3] Mishra D, Roy RB, Dutta S, Pal SK, Chakravarty D. A review on sensor based monitoring and control of friction stir welding process and a roadmap to Industry 4.0. Journal of Manufacturing Processes 2018; 36:373-397. https://doi.org/10.1016/j.jmapro.2018.10.016
- [4] Jene T, Dobman G, Wagner G, Eifler D. Monitoring of the friction stir wleding process to describe parameter effects on joint quality. Welding in the World 2008; 52:47-53. https://doi.org/10.1007/BF03266668

- [5] Fleming P, Lammlein D, Wilkes D, Fleming K, Bloodworth T, Cook G, Strauss A, DeLapp D, Lienert T, Bement M, Prater T. Inprocess gap detection in friction stir welding. Sens Rev 2008; 28(1):62–7. https://doi.org/10.1108/02602280810850044
- [6] Ramulu PJ, Narayanan RG, Kailas SV, Reddy J. Internal defects and process parameter analysis during friction stir welding of Al 6061 sheets. Int J Adv Manuf Technol 2013;65:1515–28. https://doi.org/10.1007/s00170-012-4276-z
- [7] Kumar U, Yadav I, Kumari S, Kumari K, Ranjan N, Kesharwani RK, et al. Defect identification in friction stir welding using discrete wavelet analysis. Adv Eng Softw 2015;85:43–50. https://doi.org/10.1016/j.advengsoft.2015.02.001
- [8] Kumari S, Jain R, Kumar U, Yadav I, Ranjun N, Kumari K, et al. Defect identification in friction stir welding using continuous wavelet transform. J Intell Manuf 2016; pp 1-12. DOI:10.1007/s10845-016-1259-1
- [9] Das B, Pal S, Bag S. A combined wavelet packet and Hilbert-Huang transform for defect detection and modelling of weld strength in friction stir welding process. Journal of Manufacturing Processes 2016; 22:260-268. http://dx.doi.org/10.1016/j.jmapro.2016.04.002
- [10] Boldsaikhan E, Corwin EM, Logar AM, Arbegast WJ. The use of neural network and discrete Fourier transform for real-time evaluation of friction stir welding. Appl Soft Comput 2011; 11:4839–46. https://doi.org/10.1016/j.asoc.2011.06.017
- [11] Balasubramanian N, Mishra R, Krishnamurthy K. Process forces during friction stir channeling in an aluminum alloy. J Mater Process Technol 2011; 211:305–311. https://doi.org/10.1016/j.jmatprotec.2010.10.005
- [12] Balasubramanian N, Gattu B, Mishra RS. Process forces during friction stir welding of aluminium alloys. Science and Technology of Welding and Joining 2009; 14(2):141-145. https://doi.org/10.1179/136217108X372540
- [13] Ji L, Zuo DW, Wang M. Force response characteristics and mechanical properties of friction stir welded AA2024 sheets. Mater Sci Technol 2106; 32(18):1–7. https://doi.org/10.1080/02670836.2016.1149916
- [14] Yan JH, Sutton MA, Reynolds AP. Processing and banding in AA2524 and AA2024 friction stir welding. Science and Technology of Welding and Joining 2007; 12(5): 390-401. DOI: 10.1179/174329307X213639
- [15] Boldsaikhan E, McCoy M. Analysis of tool feedback forces And material flow during friction stir welding. In: Mishra R, Mahoney MW, Sato Y, Hovanski Y, Verma R, editors. Friction stir welding and proceeding VII. Wiley, New Jersey; Wiley; 2013, p. 311–320.
- [16] Zaeh MF, Gebhard P. Dynamical behaviour of machine tools during friction stir welding. Prod. Eng. Res. Devel. 2010; 4:615–624. DOI: 10.1007/s11740-010-0273-y
- [17] Panzer F, Werz M, Welhe S. Experimental investigation of the friction stir welding dynamics of 6000 series aluminum alloys. Production Engineering 2018; 12:667–677. https://doi.org/10.1007/s11740-018-0834-z
- [18] Shrivastava A, Zinn MR, Duffie, NA, Ferrier NJ, Smith CB, Pfefferkorn FE. Force measurement-based discontinuity detection during friction stir welding. Journal of Manufacturing Processes 2017; 26:113–121. https://doi.org/10.1016/j.jmapro.2017.01.007
- [19] Shrivastava A, Pfefferkorn FE, Duffie NA, Ferrier NJ, Smith CB, Malukhin K, et al. Physics-based process model approach for detecting discontinuity during friction stir welding. Int J Advanced Manuf Technol 2015;79:604– 615. https://doi.org/10.1007/s00170-015-6868-x
- [20] Franke D, Rudraraju S, Zinn M, and Pfefferkorn FE. Understanding process force transients with application towards defect detection during friction stir welding of aluminum alloys. Journal of Manufacturing Processes 2020;54:251-261. https://doi.org/10.1016/j.jmapro.2020.03.003
- [21] Shultz EF, Cole EG, Smith CB, Zinn MR, Ferrier NJ, Pfefferkorn FE. Effect of Compliance and Travel Angle on Friction Stir Welding With Gaps. Journal of Manufacturing Science and Engineering 2010. 132:0410101-0410109.
- [22] Franke DJ, Zinn MR, Pfefferkorn FE. Intermittent Flow of Material and Force-Based Defect Detection During Friction Stir Welding of Aluminum Alloys. In: Hovanski Y, Mishra R, Sato Y, Upadhyay P, Yan D, Editors. Friction Stir Welding and Processing X. The Minerals, Metals & Materials Series. Springer, Cham; 2019, p. 149-160. https://doi.org/10.1007/978-3-030-05752-7_14
- [23] Yuquing M, Liming K, Fencheng L, Qiang L, Chunping H, Xing L. Effect of tool pin eccentricity on microstructure and mechanical properties in friction stir welded 7075 aluminum alloy thick plate. Materials and Design 2014;62:334-343. http://dx.doi.org/10.1016/j.matdes.2014.05.038